VOL. 13, NO. 1, JANUARY 2018 ISSN 1819-6608
ARPN Journal of Engineering and Applied Sciences

www.arpnjournals.com

ANALYSIS OF THE BATTERY STATE OF CHARGE AND ELECTRIC GENERATOR INFLUENCE ON THE DYNAMIC CHARACTERISTIC OF HYDRO-MAGNETO-ELECTRIC REGENERATIVE SHOCK ABSORBER

Guntur Harus Laksana[1] and Syuhri Skriptyan N. H.[2]
[1]Dynamic System and Vibration Laboratory, Department of Mechanical Engineering, Institut Teknologi Sepuluh Nopember (ITS), Surabaya, Indonesia
[2]Department of Mechanical Engineering, Universitas Negeri Jember (UNJ), Jember, Indonesia
E-Mail: haruslg@me.its.ac.id

ABSTRACT

Regenerative shock absorber has been developed and investigated widely since last two decades. Several methods have been studied to acquire maximum regenerated electric power, better efficiency and to maintain its performace close to the convensional shock absorber in providing vehicle ride quality. In this paper, a novel study on the influence of battery state of charge (SOC) and electric generator properties on the dynamic characteristic of a hydro-magneto-electric-regenerative shock absorber (HMERSA) is presented. The focused study is on how the battery SOC and electric generator properties influence the damping force characteristic, the generated electricity and the efficiency of HMERSA. The battery SOC and generator were tested and the relation between current, voltage and electric torque then formulated based on the test result. The empiric formula of the electric variable were used to develop the dyanmic model of HMERSA and quarter model of the vehicle.The results are reported and discussed in this paper.

Keywords: regenerative shock absorber, battery state, charge, dynamic characteristic, damping force, electric power, regenerated energy.

INTRODUCTION

Regenerative shock absorber (RSA) is developed to recover or to regenerate the wasted vibrational energy from the suspension system of a vehicle into electrical energy. In the last decade, study on the development of RSA for vehicle suspension has been vigorously carried out. Several types of RSA and methods of regenerating the vibration energy losses into electricity are reported. Zuo [1-2], Guntur [3-4] , Gupa [6], Fang [7], Xu [8], Zhang [9], Umeda [10] and many others reported the development of RSA using mechanic-magneto-electric, hydraulic-magneto-electric and mechanic-piezoelectric methods. The focused researches are mostly on the ouput electric power that can be produced by RSA and the effect of each method to the change of damping force characterstic of the RSA.

Guntur *et al* reported the development of a regenerative shock absorber using gear transmission system and electric generator [3]. The prototype can produce electricity up to 20 Watt per suspension and its characteristics were experimentaly investigated. The result shows that its characteristics are mainly affected by the gear system which close to dry friction damper. In further research, Guntur *et al* [4] studied the influence of hydraulic cylinder dimater to the total damping force and the generated electricity of hydro-regenerative absorber. And in advance, Guntur [5] studied the influence of asymmetry ratio and average of the damping force on the performance and ride comfort of a vehicle. From the two article, Guntur reported that there is a significant different of damping force characteristic beween conventional-viscous shock absorber and RSA. In his study, Guntur has not utilised battery and considered the change in generator characteristics. Xu *et al* [8] evaluated the strength and weakness of several kinds of energy-regenerative shock absorbers. Xu proposed a Hydraulic Energy-Regenerative Shock Absorber (HESA) and analyzed the damping characteristic and the regenerated electrical energy of the HESA. Suda *et al* [11] developed a self-powered active suspension using a linear DC motor which acted as actuator and regenerative absorber. Zuo *et al* [1] developed a linear electromagnetic shock absorber using permanent magnet and conductor coil. The 1:2 scale prototype was able to produce 16-64W power at 0.25-0.5 m/s RMS suspension velocity. By combining permanent magnetic generator and rack-pinion mechanism, Li *et al* [12-13] developed a regenerative shock absorber with variable damping. Using rack-pinion mechanism and one way bearing, Guntur [3] and Li [13] convert oscillatory vibration into unidirectional motion of electric generator, which produce better effiecy and performance at high frequency. Yu *et al* [14] utilised two overrunning clutches and planetary gear to drive a generator, which can realize similar function.Guo *et al* [14] patented a hydraulic regenerative shock absorber for vehicle suspension which can harvest the vibration energy and improve ride comfort. As RSA consists of mechanical and electrical system, the total damping force characteristics and the regenerated electric power will be influenced by its mechanical and electrical damper characteristics. Study on the influence of electrical properties to the dynamic characteristic of the RSA, such as battery state of charge (SOC) and electric generator utilised in the RSA are also very important to be done to acquire high performance of suspension and vehicle ride comfort. In this paper, a novel study on the influence of battery state of charge (SOC) and electric

generator properties on the dynamic characteristic of a regenerative shock absorber (RSA) is presented and discussed. The focused study is on how the SOC and electric generator properties influence the damping force characteristic, the generated electricity and the efficiency of RSA.

RESEARCH METHOD

The research was started by literuature study, designing the prototype of HMERSA, electrical system test, gevorning the dynamic equation-modelling and simulation, and model validation.

Regenerative shock absorber design and prototype

Figure-1 shows the design image of the HMERSA and Figure-2 shows the prototype. The HMERSA is mainly consist of hydraulic cylinder, flexible tube, hydraulic motor and electric generator having maximum ouput power of 100Watt. The principle of work of the HMERSA is converting the relative displacement of the vehicle suspension to unidirectional fluid flow into the hydraulic motor and drive the electric generator to produce electricity. The generated electricity is rectified and amplified using diode and DC step up, respectively before being charged to the battery. In this prototype, the specification of battery/accumulator is 12V 5Ah, as seen in the schematic image in Figure-3.

Theoretical background and system modelling

The prototype of HMERSA consists of mechanical and electrical system. This mechanical and electrical system will produce mechanical and electrical damper. The mechanical damper depends on the design of the hydraulic cylinder diameter, oil viscousity and the existing head loss, while the electrical damper is affected by the electric generator characteristics and battery state of charge (SOC).

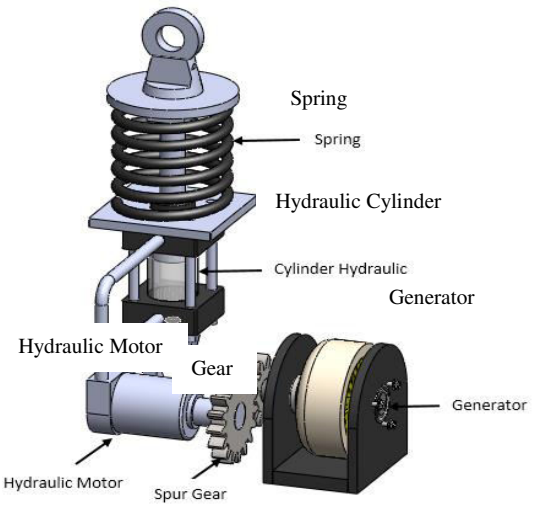

Figure-1. Design image of HMERSA.

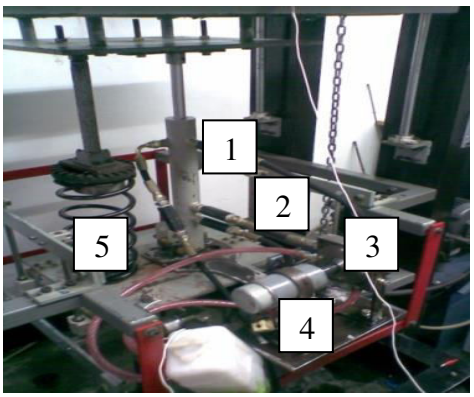

Figure-2. Prototype of HMERSA: 1.Hydarulic cylinder; 2.Flexible tube; 3.Hydarulic motor; 4.Generator; 5.Spring.

As seen in Figure-3, the mechanical damping force will be influenced by the cylinder-pipe system pressure drop and the efective cross sectional area of the hydraulic cylinder. The cylinder-tube system pressure drop defined by equation (1) and (2).

(a) expansion

$$\Delta P_{ct} = \frac{\rho}{2}\left(\left(\frac{A_{11}}{A_{cv}}\right)^2 - 1\right)v^2 \quad (1)$$

(b) compression

$$\Delta P_{ct} = \frac{\rho}{2}\left(\left(\frac{A_{12}}{A_{cv}}\right)^2 - 1\right)v^2 \quad (2)$$

with ρ: oil density, A: cylinder/tube area, v: fluid velocity. Based on the continuity equation, the relation between tube velocity (v_t) and hydraulic cylinder velocity (v_c) can be found, as follows:

$$v_t = \frac{A_c}{A_t}v_c \quad (3)$$

Pressure drop due to tube head loss (ΔP_t) is expressed by: (4.1)

$$\Delta P_t = \rho\left(32\mu\frac{Lv_t}{\rho {D_t}^2} + k\frac{v_t^2}{2}\right) \quad (4)$$

Substituting equation (3) into (4), pressure drop due to pipe head loss can be written as:

(a) expansion:

$$\Delta P_t = \frac{8.A_{11}}{\pi^2.{D_t}^4}(16.\mu.\pi.L.v + k.\rho.A_{11}.v^2) \quad (5)$$

(b) compression

$$\Delta P_t = \frac{8.A_{12}}{\pi^2.{D_t}^4}(16.\mu.\pi.L.v + k.\rho.A_{12}.v^2) \quad (6)$$

with L: pipe/tube length, μ:oil viscousity. Angular velocity and torque of the hydarulic motor in HMERSA are obtained by the following equaitons:

$$\omega = \frac{Q_{hm}}{q}\eta_v \quad (7)$$

$$T_{hm} = \Delta P_{hm}.q.\eta_m \quad (8)$$

with T_{hm}:pipe/tube length, μ:oil viscousity, Q_{mh}: flow rate, η_v:volumetric efficiency, q:motor displacement. As mechanical torque is defined by multiplication of inertia (J) and angular acceleration ($\dot{\omega}$) :

$$T = J.\dot{\omega} \quad (9)$$

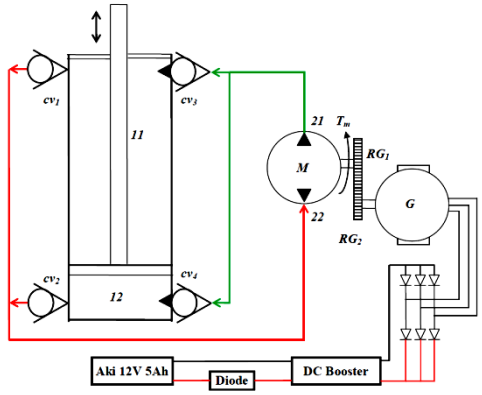

Figure-3. Schematic image of HMERSA with electrical circuit.

Substituting equation (7), (8) into (9), pressure drop in the hydraulic motor (ΔP_{hm}) can be written as:

$$\Delta P_{hm} = \frac{J.\eta_v}{\eta_m.q^2}\dot{Q}_{hm} \quad (10)$$

(2.4)

One gear pair within the hydarulic motor which connect the hydraulic system with the electric generator will influence the damping force of the HMERSA and their mehcanical torque can be derived by the following equations:

$$J_1\ddot{\theta}_1 + \frac{r_1}{r_2}\left[J_2\ddot{\theta}_2 + T_e\right] = T_m \quad (11)$$

$$(J_1 + J_2N^2)\ddot{\theta}_1 + T_e.N = T_m \quad (12)$$

with T_e:electric torque induced by generator, J_1:gear 1 moment of inertia, J_2:gear 2 moment of inertia, N:number of teeth.Substituting equation (11), (12) into equation (10), the hydraulic motor's pressure drop is shown in the following equations:

(a) expansion:

$$\Delta P_{hm,exp} = \frac{(J_1+J_2N^2).\eta_v.A_{11}}{\eta_m.q^2}\dot{v} + \frac{k_t.k_m.\eta_v.N^2.A_{11}}{(R_{in}+R_{ex})\eta_m.q^2}v \quad (13)$$

(b) compression: (4.2)

$$\Delta P_{hm,comp} = \frac{(J_1+J_2N^2).\eta_v.A_{12}}{\eta_m.q^2}\dot{v} + \frac{k_t.k_m.\eta_v.N^2.A_{12}}{(R_{in}+R_{ex})\eta_m.q^2}v \quad (14)$$

And the expansive and compressive damping force of the HMERSA are defined by the following equations:

(a) expansion

$$F_{D,e} = \frac{\rho}{2}\left(\left(\frac{A_{11}}{A_{cv}}\right)^2 - 1\right)v^2 + \frac{8.A_{11}}{\pi^2.D_p^4}(16.\mu.\pi.L.v + k.\rho.A_{11}.v^2)$$

$$+\frac{(J_1+J_2N^2).\eta_v.A_{11}}{\eta_m.q^2}\dot{v} + \frac{k_t.k_m.\eta_v.N^2.A_{11}}{(R_{in}+R_{ex})\eta_m.q^2}v \quad (15)$$

(b) compression

$$F_{D,c} = \frac{\rho}{2}\left(\left(\frac{A_{12}}{A_{cv}}\right)^2 - 1\right)v^2 + \frac{8.A_{12}}{\pi^2.D_p^4}(16.\mu.\pi.L.v + k.\rho.A_{12}.v^2)$$

$$+\frac{(J_1 + J_2N^2).\eta_v.A_{12}}{\eta_m.q^2}\dot{v} + \frac{k_t.k_m.\eta_v.N^2.A_{12}}{(R_{in} + R_{ex})\eta_m.q^2}v \quad (16)$$

The DC generator shown in Figure-3 can be modeled as RL Circuit. Owing to Kirchoff law, the following equation is obtained:

$$L\frac{di}{dt} + R.i + R_{Load}.i = E_m.\dot{\theta}_2 \quad (17)$$

And the electric torque is:

$$T_e = \frac{V.i}{\dot{\theta}_2} \quad (18)$$

with electrique torque (T_e), voltage (V) and current (i) are defined by the equations acquired from the electrical system characteristics test.

The quarter car model of vehicle with HMERSA is seen in Figure-4. Owing to the newton second law of motion, the quarter car model equation of motion due to road excitation is shown by equation (19), with the damping force (F_d), which is proportional to the total pressure drop and hydraulic system effective area (A).

$$m\ddot{x} + k(x - y) + F_d = 0 \quad (19)$$

Electrical system test

The electrical system of the HMERSA consists of generator, rectifier circuit, DC voltage step up circuit, diode and battery/accumulator. To investigate the influence of generator and battery state of charger (SOC), the following test was conducted. Figure-5 shows the schematic diagram of the electrical system characteristic test. Input velocity (ω_i) to the generator was defined and varied within the suspension operating range of frequency, i.e. from 36 rpm to 630 rpm.The test was conducted at various battery state of charger (SOC): 25%, 50%, 75% and 100%. The ouput voltage and current were measured for each input velocity and battery SOC.

Table-1. Mechanical parameters of HMERSA.

Parameter	Notation	Value	Unit
Hydarulic cylinder and piping system			
Piston bore diameter	D_b	32	cm
Piston rod diameter	D_r	18	cm
Check valve effective diameter	D_{cv}	3/8	Inch
Pipe diameter	D_p	3/8	Inch
Panjang pipa total	L	1,75	m
Konstanta *head loss minor*	k	12,04	
Hydarulic motor (BMM-8)			
Displacement	q	8,2	cc/rev
Mechanics efficiency	η_m	0,90	
Volumetric efficiency	η_v	0,75	
Hydarulic fluid (ISO VG 10)			
Kinematic viscousity	μ	10	mm^2/s
Oil density	ρ	846	kg/m^3
Gear			
Gear-1 diameter	D_{RG1}	115	mm
Gear-1 mass	m_{rg1}	0,343	kg
Gear-2 diameter	D_{RG2}	45	mm
Gear-2 mass	m_{rg2}	0,058	kg

Table-2. Electrical parameters acquired from the test result linear approximation.

SOC (%)	**Voltage** (V)			
	$0 \leq \omega \leq 130$		$\omega > 130$	
	α	A	α	A
25	0.179	-10.4598	0.0036	11.8
50			0.0061	11.4
75			0.0033	11.8
100			0.0041	11.7
SOC (%)	**Current** (i)		**Electric Torque** (T_e)	
	$\omega > 130$		$\omega > 130$	
	β	B	C_{Te}	ε
25	0.0035	-0.570	$7.25.10^{-4}$	-0.094
50	0.0039	-0.648	$9.14.10^{-4}$	-0.118
75	0.0043	-0.738	$9.16.10^{-4}$	-0.119
100	0.0037	-0.616	$7.98.10^{-4}$	-0.103

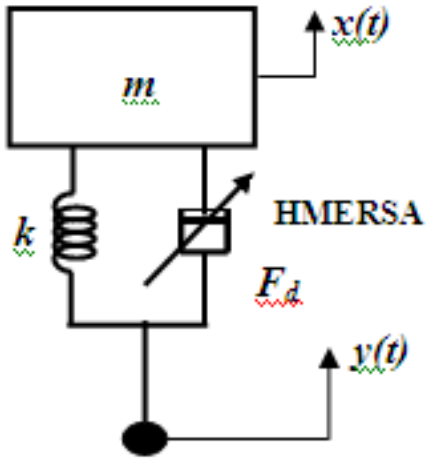

Figure-4. Quarter car dynamic model with HMERSA.

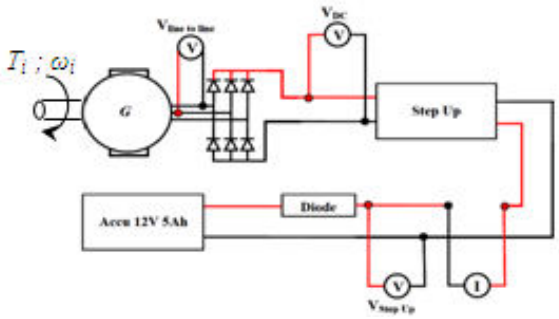

Figure-5. Schematic diagram of the electrical system characteristic test.

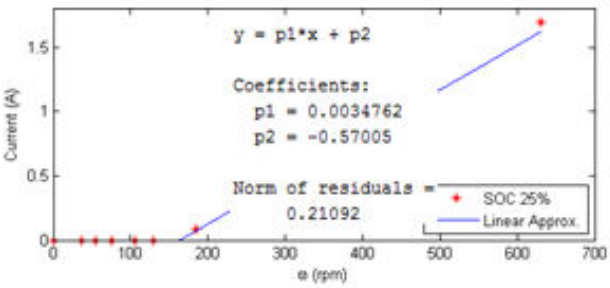

Figure-6. Test result and linear approximation of the generator's electric **c**urrent at SOC 25%.

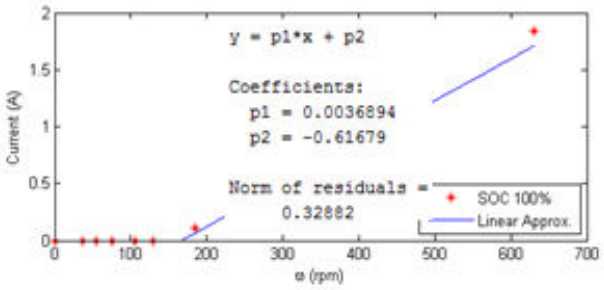

Figure-7. Test result and linear approximation of the generator's electric current at SOC 100%.

RESULT AND DISCUSSIONS

Electrical system test results

Figure 6 to 11 show the plotted results and the trend line approximation for current, voltage and torque of the generator as a function of input velocities at various battery SOC.It is seen that when the generator ouput voltage ($V_{L\text{-}L}$) less than 2.5 volt, the DC voltage step up circuit can not produce the required minimum voltage to charge the battery (12volt), as can be seen that $V_{step\text{-}up}$ remain the same with $V_{L\text{-}L}$ and no current flows to the battery ($I=0$). However, when the output voltage ($V_{L\text{-}L}$) over 2.5 volt, the voltage is stepped up into the required minimum voltage to charge the battery, i.e. over 12 volt and current flows to the battery. Based on the output voltage, current and the input velocity, the electric torque (T_e) for various input velocities and battery SOC can be calculated.

The linearized ouput voltage, current and electric torque of the generator as a function of input velocities can be written into equation (20), (21) and (22), with conditions and constants defined in Table 2.

$$V = \alpha.\omega + A \quad (20)$$

$$i = \beta.\omega + B \quad (21)$$

$$T_e = C_{Te}.\omega + \varepsilon \quad (22)$$

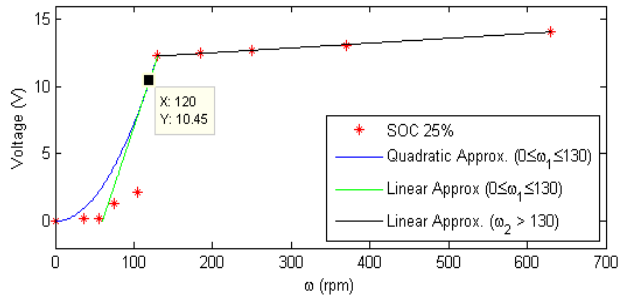

Figure-8. Test result and linear approximation of the generator's electric votage at SOC 25%.

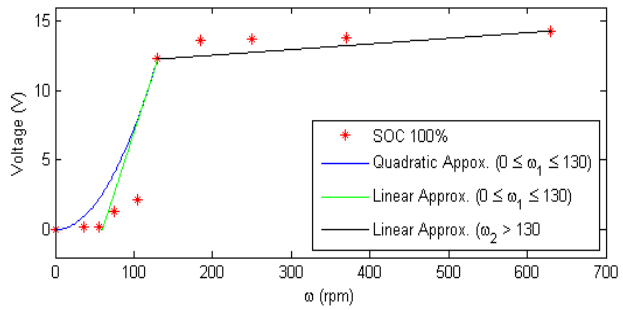

Figure-9. Test result and linear approximation of the generator's electric votage at SOC 100%.

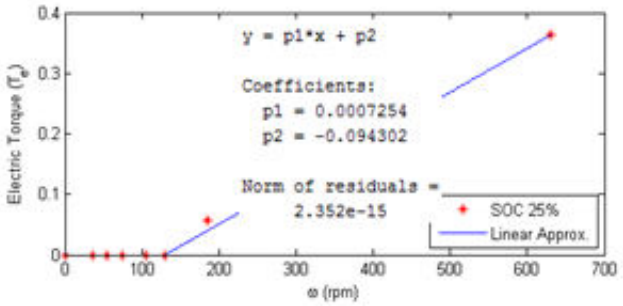

Figure-10. Test result and linear approximation of the generator's electric torque at SOC 25%.

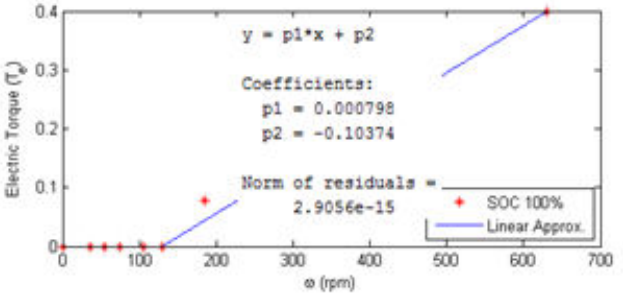

Figure-11. Test result and linear approximation of the generator's electric torque at SOC 100%.

The influence of battery SOC to the HMERSA

Figure-12 shows the generator's damping force versus displacement and velocity for various battery SOC (25%, 50%, 75% and 100%), while Figure-13 shows the HMERSA's total damping force at various battery SOC. This results show the influence of battery SOC to the total damping force of the system. Battery SOC significantly influences the damping force and energy absorbtion capacity of the shock absorber. As shown in the figure, 25% battery SOC (almost empty) has the lowest ability to absorb the vibration energy, which means lower damping force.Likewise, 100% battery SOC (fully charged) also produce lower ability to the system to absorb energy. In between 25% and 100%, the ability to absorb energy is much higher, as shown by 50% and 75% battery SOC.

The ouput current, voltage and power of the HMERSA for various battery SOC can be seen in figure 14 to 16. As can be seen in the figures, the ouput voltage, current and power are higher for battery SOC of 50% and 75%, as compared to 25% and fully charged 100%. As shown in Figure-28, the battery SOC does not influence the efficiency of the HMERSA significantly.

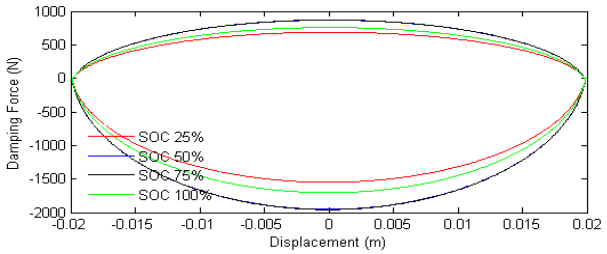

(a)

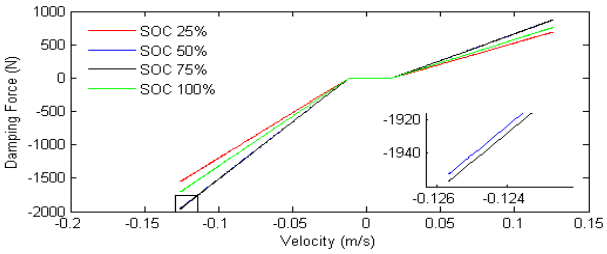

(b)

Figure-12. Generator's damping force at various SOC. (a) Damping force vs displacement; (b) Damping force vs velocity.

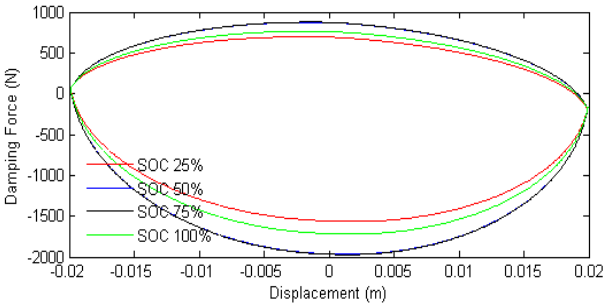

(a)

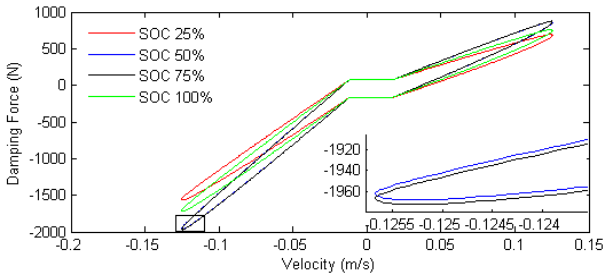

(b)

Figure-13. HMERSA's damping force at various SOC. (a) Damping force vs displacement; (b) Damping force vs velocity.

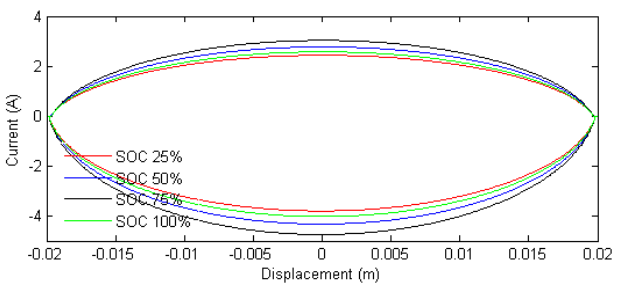

(a)

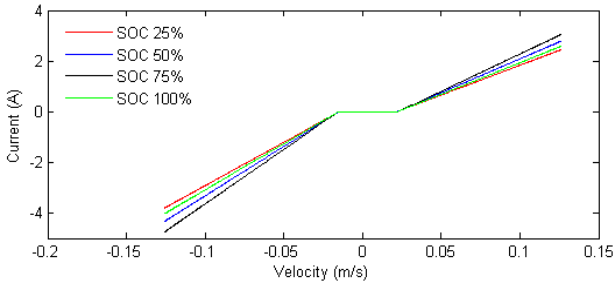

(b)

Figure-14. Generator's current at various SOC. (a) Current vs displacement; (b) Current vs velocity.

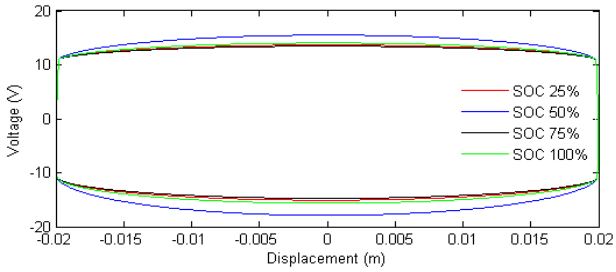

(a)

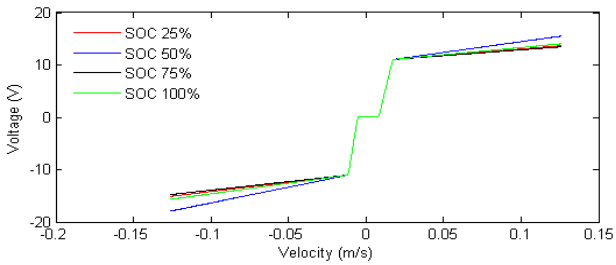

(b)

Figure-15. Generator's voltage at various SOC. (a) Voltage vs displacement; (b) Voltage vs velocity.

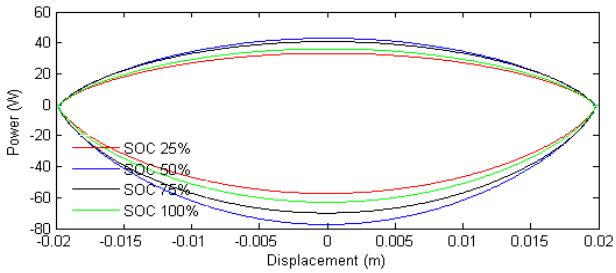

(a)

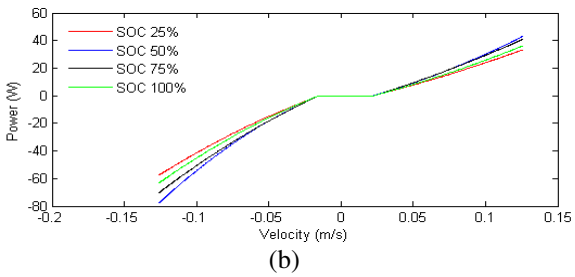

(b)

Figure-16. Generator's power at various SOC. (a) Power vs displacement; (b) Power vs velocity.

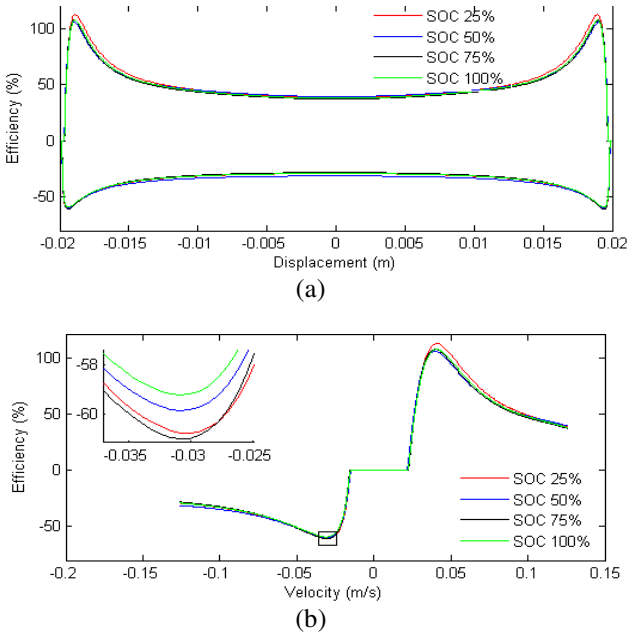

Figure-17. HMERSA's power efficiency at various SOC. (a) Efficiency vs displacement; (b) Efficiency vs velocity.

Simultaneous influence of battery SOC and Generator's maximum power

Figure-18 shows the simultaneous influence of generator maximum power and SOC on the dynamic response of sprung mass and damping force: (a) Sprung mass displacement vs generator maximum power-SOC; (b) Sprung mass acceleration vs generator maximum power-SOC; (c) Sprung mass displacement vs generator maximum power-SOC. It is shown that the displacement and acceleration are similar, i.e. at battery SOC near empty 0%-25% and close to fully charged 100%, the displacement and accerelaration are both high. Inversely, at battery SOC : 25% < SOC < 100%, the displacement and acceleration are low due to higher damping force or enegy absorbtion capacity of the shock absorber. The results show that using higher spec of generator maximum power will increase the damping force and hence reduce the displacement and acceleration responses of the sprung mass.

Figure-19 shows the simultaneous influence of generator maximum power and SOC on the generated electrcity of HMERSA: (a) Ouput current vs generator maximum power-SOC; (b) Output voltage vs generator maximum power-SOC; (c) Ouput power vs generator maximum power-SOC. It is shown that the ouput current from the generator is influenced by the battery SOC, but not for the ouput voltage. When the battery is fully charged, current difficult to flow into the battery, which means low current, as seen in figure 18 and hence producing high damping force to the HMERSA. Inversely, when the battery is empty, the current can be easily flow into the battery and hence produce lower damping force. The ouput voltage is proportional to the generator maximum power. Higher voltage produced at higher generator maximum power. The ouput power shows that HMERSA can generate higher electric power at lower SOC (empty state) and at higher generator maximum power.

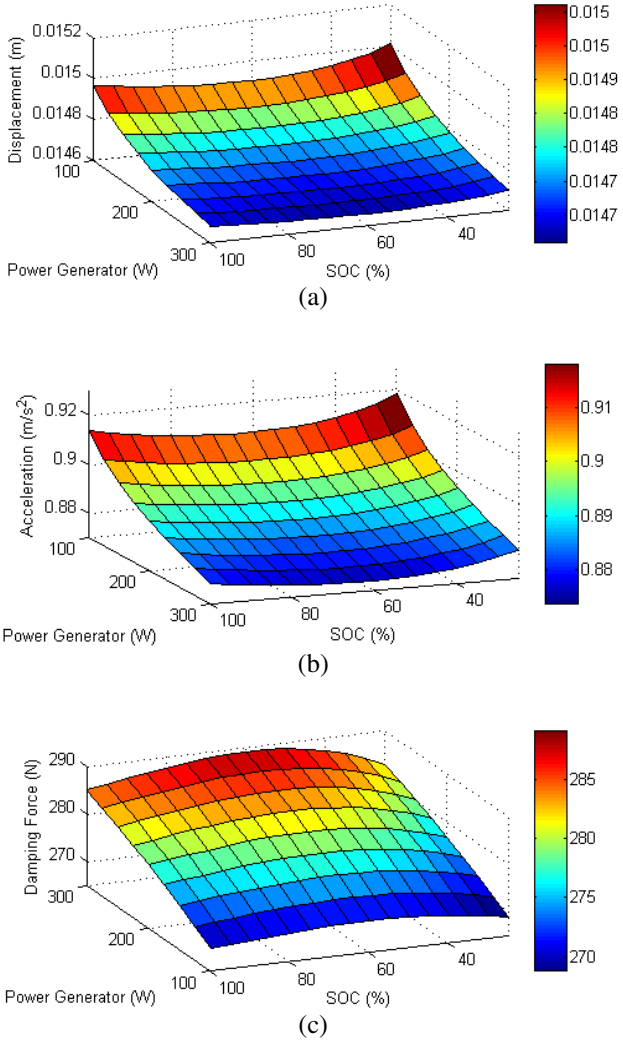

Figure-18. The influence of SOC and generator's power on the dynamic response of sprung mass and damping force.(a) Sprung mass displacement vs generator maximum power-SOC; (b) Sprung mass acceleration vs generator maximum power-SOC; (c) Sprung mass displacement vs generator maximum power-SOC.

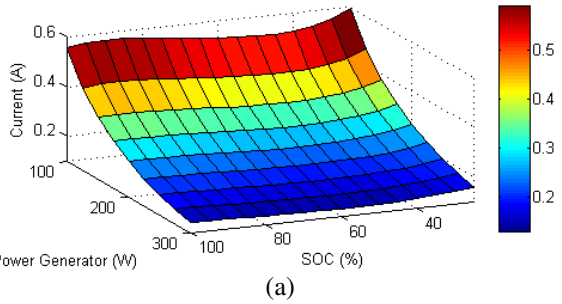

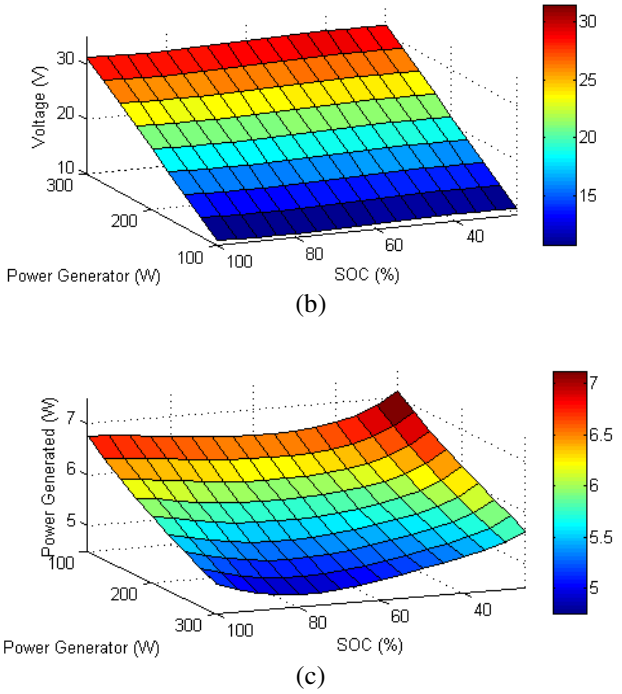

Figure-19. Simultaneous influence of generator maximum power and SOC on the output electricity.(a) Current vs generator maximum power-SOC; (b) Voltage vs generator maximum power-SOC; (c) Generated power vs generator maximum power-SOC.

Figure 20(a)-(b) shows how the mechanical and electrical damping force of HMERSA change as the generator maximum power and bateery SOC change. The influence of generator maximum power and battery SOC to the effiency of HMERSA is presented in figure 20(c). The results show a reverse phenomena between mechanical and electrical damping. The efficiency of the HMERSA is influenced by the generator maximum power and battery SOC,which is high for lower generator maximum power and lower battery SOC.

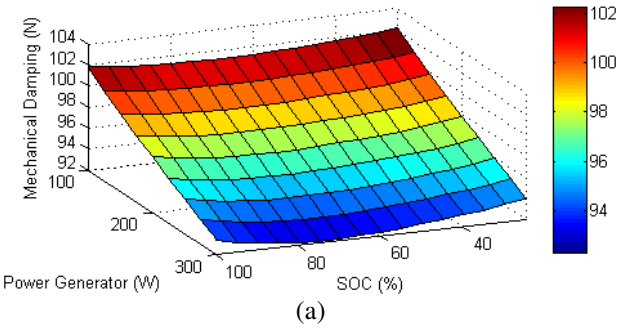

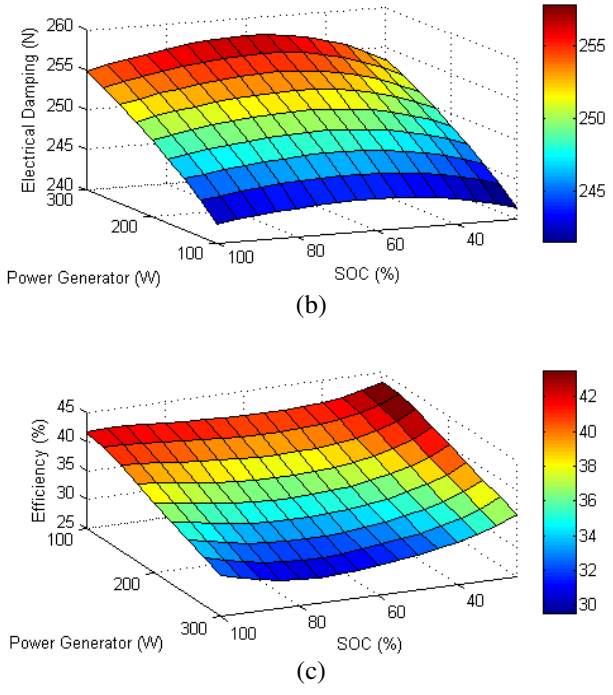

Figure-20. Simultaneous influence of generator maximum power and SOC on the output electricity.(a) Current vs generator maximum power-SOC; (b) Voltage vs generator maximum power-SOC; (c) RMS power vs generator maximum power-SOC.

SUMMARY

Generator maximum power and battery SOC have significant influence on the energy absorbtion capacity and the total damping force of shock absorber. Inversily, they do not influence the efficiency of the shock absorber significantly.The shock absorber's ouput current and power are influenced by the battery SOC. The ouput is higher when the battery SOC near empty 0%-25% and close to fully charged 100%. However,the output voltage is not influenced significantly. When the battery is fully charged, current is difficult to flow into the battery, means low current, and hence produce high damping force to the shock absorber. Inversely, when the battery is empty, current can be easily flow into the battery and hence produce lower damping force.The vehicle sprung mass displacement and acceleration show similar phenomena, high when the battery SOC near empty 0%-25% and close to fully charged 100%.

ACKNOWLEDGEMENT

This research is part of research funded by DRPM (Direktorat Riset dan Pengabdian Masyarakat)-RISTEKDIKTI, through scheme of Penelitian Unggulan Perguruan Tinggi (PUPT) 2017.

REFERENCES

[1] Lei Zuo, B. Scully, J. Shestani and Y.Zhou. 2010. Design and Characterization of an Electromagnetic

Energy Harvester for Vehicle Suspensions. Smart Materials and Structures. 19(4).

[2] Lei Zuo, Pei Seng Zhang. 2013. Energy Harvesting, Ride Comfort, and Road Handling of Regenerative Vehicle Suspension. ASME Journal of Vibration and Acoustics. 135(1): 011002-01002-8.

[3] Harus Laksana Guntur, Wiwiek Hendrowati, Rahman Roy Lubis. 2013. Development and Analysis of a Regenerative Shock Absorber for Vehicle Suspension. JSME Journal of System Design & Dynamics. 7(3): 304-315.

[4] Harus Laksana Guntur. 2016. Analysis of the Influence of Hydraulic Cylinder Diameter to the Total Damping Force and the Generated Electricity of Regenerative Shock Absorber. ARPN Jurnal of Engineering and Applied Science. 11(2): 873-878.

[5] Harus Laksana Guntur, Listy Fazria Setiawan. 2016. The Influence of Asymmetry Ratio and Average of the Damping Force on the Performance and Ride Comfort of a Vehicle. International Journal of Vehicle System Modelling and Testing. 11(2): 97-115.

[6] A.Gupa, J.A. Jendrzejcyk, T.M. Mulchany and J.R. Hull. 2006. Design of Electromagnetic Shock Absorber. International Journal of Mechanics and Materials in Design. 3(3): 285-291.

[7] Zhigang Fang, Xuexun Go, Lin Xu, Han Zang. 2013. Experimental Study of Damping and Energy Regeneration Characteristics of Hydraulic Electromagnetic Shock Absorber. Advances in Mechanical Engineering. pp. 1-9.

[8] Lin Xu, Xubo Li, Xiaowei Hu, Bian Gong. 2013. Performance Simulation of Hydraulic Electromagnetic Shock Absorber. Advanced Materials Research. 798-799: 382-385.

[9] Yuxin Zhang, Xinjie Zhang, Min Zhan, Konghui Guo, Fuquan Zhao, Zongwei Liu. 2014. Study on a Novel Hydraulic pumping regenerative suspension for vehicles. Journal of the Franklin Institute-Elsevier. pp. 1-15.

[10] Umeda M., Nakamura K. And Ueha S. 2014. Analysis of Transformation of Mechanical Impact Energy to Electric Energy using Piezoelectric Vibrator. Japan Journal of Applied Physiscs. Vol. 3B, 3267-3273 (1996). Les. Journal of the Franklin Institute-Elsevier. pp. 1-15.

[11] Yoshihiro Suda, Shigeyuki Nakadai, Kimihiko Nakano. 1998. Hybrid Suspension System with Skyhook Control and Energy Consumption and Vehicle Maneuver. Vehicle System Dynamic. 29(S1): 619-s634.

[12] Z.J. Li, L.Zuo, G. Luhrs, L.J. Lin, Y.X. Qin. 2013. Electromagnetic Energy Harvesting Shock Absorbers Design, Modeling, and Road Tests. IEEE Trans. Vehicle Technology. 62(3): 1065-1074.

[13] Z.Li, L.Zuo, J.Kuang, G.Luhrs. 2013. Energy-Harvesting Shock Absorber with a Mechanical Motion rectifier. Smart Material Structure. 22(2): 025008.

[14] C.Yu, S.Rakheja, W.Wang, Q.Wang. 2013. Analysis of an on-off Regenerative Electromechanical Damper. Proc. Institute of Mechanical Engineering, Part D: Journal of Automobile Engineering. 227(5): 704-722.

[15] K.H. Guo, Y.X. Zhang, Y.H. Chen, Y.Liu. 2013. Pumping Shock Absorber and Hydraulically Interconnected Regenerative Active Vehicle Suspension, CN Patent 2013 104 413 672.